Engineering Science and Technology, an International Journal 18 (2015) 503–511

HOSTED BY

Contents lists available at ScienceDirect

Engineering Science and Technology, an International Journal

journal homepage: http://www.elsevier.com/locate/jestch

Full length article

Lattice Boltzmann simulation of natural convection in an L-shaped enclosure in the presence of nanofluid

Bouchmel Mliki [a], Mohamed Ammar Abbassi [a,*], Kamel Guedri [b], Ahmed Omri [a]

[a] UR: Unité de Recherche Matériaux, Energie et Energies Renouvelables (MEER), Faculté des Sciences de Gafsa, B.P.19, Zarroug, Gafsa, 2112, Tunisia
[b] Mechanical Engineering Department, College of Engineering and Islamic Architecture, Umm Al-Qura University, Saudi Arabia

ARTICLE INFO

Article history:
Received 6 February 2015
Received in revised form
3 April 2015
Accepted 6 April 2015
Available online 7 May 2015

Keywords:
Lattice Boltzmann method
Nanofluid
Natural convection
L-shaped enclosure

ABSTRACT

In the present paper, fluid flow and heat transfer inside L-shaped enclosure filled with Cu/water nanofluid has been investigated numerically using the Lattice Boltzmann Method. The validity of the numerical code used is ascertained and good agreement was found with published results. The effects of different parameters such as Rayleigh number (10^3–10^6), aspect ratio of the L-shaped enclosure (0.2–0.6) and nanoparticle volume concentration (0–0.05) on the flow and temperature fields are studied. The obtained results show that nanofluid enhances the heat transfer amount and reducing the aspect ratio improves this effect. Also it was found that the mean Nusselt number increased with increase in Rayleigh number.

1. Introduction

Over the past few years, the Lattice Boltzmann Method (LBM) has found wide-ranging applications in science and engineering [1–3]. This surge in interest is mainly attributed to its ability of simple and efficient computational procedure, even for complex geometries [4–6]. Therefore, the LBM method is able to simulate the complicated fluid flows such as multiphase flows, chemically reacting flows, viscoelastic non-Newtonian flows. The term “nanofluid” (that is used for the first time by Choi [7]) refers to a liquid containing a dispersion of submicronic solid particles (nanoparticles). The characteristic feature of nanofluids is thermal conductivity enhancement, a phenomenon observed by Khanafer et al. [8]. It was revealed that the heat transfer rate increases with the increase of particle fraction at any given Grashof number. This is why intensive researches focus on the heat transfer augmentation utilizing nanofluids and their potential in cooling industry has been carried out recently [9–12]. There are a number of recent studies on free convection inside cavities containing nanofluid. Kahveci [13] numerically studied the heat transfer enhancement of water-based nanofluids in a differentially heated, tilted enclosure for a range of inclination angles, nanoparticle radii, solid volume fractions, and Rayleigh numbers. It was concluded from the results that suspended nanoparticles substantially increase the heat transfer rate and the average Nusselt number is nearly linear with the increase of solid volume fraction. Recently Mahmoodi et al. [14] studied the Cu/water nanofluid free convection in an L-shaped cavity using the finite volume method. They analyzed the effect of different parameters such as Rayleigh number, aspect ratio and nanoparticle volume concentration on the flow and temperature fields as well as on the average Nusselt number. They showed that average Nusselt number decreases by an increase in volume concentration, especially for higher Rayleigh numbers. Dehnavi and Rezvani [15] studied the alumina/water nanofluid free convection in a Γ-shaped cavity. Their results showed that heat transfer increases with a reduction in nanoparticle size and also with increase in parameter R (ratio of the minimum diameter to maximum diameter of the nanoparticles). In another study Kalteh and Hasani [16] investigated the nanofluid free convection in an L-shaped cavity using the LBM. Their results showed an increase in average Nusselt number with an increase in nanoparticle volume concentration, for all the considered Rayleigh numbers and aspect ratios. Mahmoudi et al. [17] studied numerically the effects of linear temperature distribution on natural convection in a square enclosure filled with a water-Al_2O_3 nanofluid under the influence of a magnetic field. They showed that magnetic field direction controls the effect of nanoparticles in the fluid. Bakier [18] numerically studied the heat transfer and fluid flow through C-shaped enclosure filled with nanofluid that has two openings and

* Corresponding author.
E-mail address: medammar.abbassi@enim.rnu.tn (M.A. Abbassi).
Peer review under responsibility of Karabuk University.

http://dx.doi.org/10.1016/j.jestch.2015.04.008

Nomenclature

c	Lattice speed
c_s	Speed of sound
c_i	Discrete particle speeds
c_p	Specific heat at constant pressure
F_i	External forces
f	Density distribution functions
f^{eq}	Equilibrium density distribution functions
g	Internal energy distribution functions
g^{eq}	Equilibrium internal energy distribution functions
$\mathbf{g}$	Gravity vector
k	thermal conductivity
Ma	Mach number
Nu	Local Nusselt number
P	Pressure
Pr	Prandtl number
Ra	Rayleigh number
T	Temperature
$\mathbf{u}(u,v)$	Velocities
$\mathbf{x}(x,y)$	Lattice coordinates

Greek symbols

a	Thermal diffusivity
Δx	Lattice spacing
Δt	Time increment
ϕ	Solid volume fraction
μ	Dynamic viscosity
ρ	Fluid density
τ_α	Relaxation time for temperature
τ_ν	Relaxation time for flow
θ	Non-dimensional temperature
ν	Kinematic viscosity
Ψ	Non-dimensional stream function

Subscript

f	fluid
nf	nanofluid
p	particle

movable heat source. Results showed that for low Rayleigh number, the addition of nanoparticles is necessary to enhance the heat and mass transfer through the opening boundaries. Mejri et al. [19] applied lattice Boltzmann method to investigate the Magnetic field effect on entropy generation in a nanofluid-filled enclosure with sinusoidal heating on both side walls. They showed that using water–Al_2O_3 nanofluid reduces the entropy generation while an increase in the Hartmann number increases the entropy generation number. Sheikholeslami et al. [20] analyzed the magneto hydrodynamic nanofluid flow and heat transfer in a concentric annulus. Their results indicated that Nusselt number has a direct relationship with nanoparticle volume fraction, Rayleigh number and it has a reverse relationship with Hartmann number. Sheikholeslami et al. [21] studied the problem of MHD free convection in a horizontal cylindrical enclosure with an inner triangular cylinder. The effect of nanoparticle volume fraction for the enhancement of heat transfer has been investigated for several sets of values of Rayleigh and Hartmann numbers. The presented results indicate that the value of the maximum stream function decreases with increasing Hartmann number. In addition, the results indicate that Nusselt number increase with increasing Rayleigh number. Sheikholeslami and Ganji [22] studied the Magnetohydrodynamic flow of CuO–water nanofluid in a square enclosure with a rectangular heated body. In this study, the effective thermal conductivity and the effective viscosity of nanofluid were calculated by KKL (Koo-Kleinstreuer-Li) correlation. The results of this study show that the heat transfer rate and dimensionless entropy generation number increase with increase of the Rayleigh number and nanoparticle volume fraction but it decreases with increase of the Hartmann number. MHD effect on natural convection heat transfer in an enclosure filled with nanofluid was studied by Sheikholeslami et al. [23]. They found that effect of Hartmann number and heat source length is more pronounced at high Rayleigh number. MHD free convection in an eccentric semi-annulus filled with nanofluid was studied by Sheikholeslami et al. [24]. The effective thermal conductivity and viscosity of nanofluid were calculated by the Maxwell–Garnetts (MG) and Brinkman models, respectively. They found that Nusselt number has direct relationship with nanoparticle volume fraction and Rayleigh number but it has inverse relationship with Hartmann number and position of inner cylinder at high Rayleigh number. Effect of thermal radiation on magnetohydrodynamics nanofluid flow between two horizontal rotating plates was studied by Sheikholeslami et al. [25]. The effects of Reynolds number, magnetic parameter, rotation parameter, Schmidt number, thermophoretic parameter, Brownian parameter and radiation parameter on heat and mass characteristics has been investigated. They demonstrated that the concentration boundary layer thickness decreases with the increase of radiation parameter. Ellahi [26] conducted a numerical study of the MHD flow of non-Newtonian nanofluid in a pipe. He observed that the MHD parameter decreases the fluid motion and the velocity profile is larger than that of temperature profile even in the presence of variable viscosities. Hussein et al. [27] investigated numerical natural convection in an open enclosure filled with Cu–water nanofluid in the presence of magnetic field. They demonstrated that when the magnetic field orientation angle increases, the flow circulation intensity and the convection effect begin to decrease. Kefayati [28] studied the effect of an external magnetic source on natural convection flow in a cavity with linearly temperature distribution which is subjugated to kerosene/cobalt ferrofluid using Lattice Boltzmann method. It emerged that the heat transfer decreases by the increment of the nanoscale ferromagnetic particle volume fraction for various Rayleigh numbers. Rahman et al. [29] numerically studied unsteady natural convection heat transfer in an isosceles triangular enclosure filled with Al_2O_3 nanoparticle. They found that the addition of the nanoparticle into the base fluid (water) affects both heat transfer and fluid flow and deduced that heat transfer is increased with the addition of nanoparticle for all Rayleigh number investigated. Mahmoudi et al. [30] analyzed the MHD natural convection heat transfer nanofluids-filled open cavity with non uniform boundary condition in the presence of uniform heat generation/absorption by using lattice Boltzmann method. The study was carried out by using physical flow governing parameters, such as, Rayleigh number (10^3–10^6), Hartmann number (Ha = 0–60), heat generation/absorption coefficient (q = −10,−5,0,5,10) and the solid volume fraction of nanoparticles between $\phi = 0$ and 6%. The results of this study indicated the decrease in heat transfer rate with Hartmann number and linear variation with Rayleigh number. Swati and Iswar [31] investigated the effects of velocity slip and thermal slip on MHD boundary layer mixed convection flow and heat transfer. The results of this study indicated the decrease in heat transfer rate with the increasing values of thermal slip. Kefayati [32,33] simulated natural convection in an open cavity with magnetic field, a cavity with sinusoidal temperature distribution, and also turbulent natural convection. Sheikholeslami et al. [34–41] took the simulations of natural convection considering different kind of nanoparticles, and the effects of magnetic field.

This paper aims to use the lattice Boltzmann method to simulate the nanofluid free convection heat transfer in an L-shaped cavity. The effects of the Rayleigh number, aspect ratio and volume concentration on the flow and heat transfer characteristics have been examined.

2. Mathematical formulation

2.1. Problem statement and governing equations

Fig. 1 depicts the schematic view of the considered problem. It consists of an L-shaped enclosure with H as height and W as width (H = W) and the thickness is L. The aspect ratio of the enclosure is defined as AR = L/H. The hot walls (ABC), the cold walls (DEF) and the adiabatic walls (AF and CD) are shown in this figure. The cavity is filled with Cu/water nanofluid that is considered to be Newtonian, laminar and incompressible. Moreover, the nanofluid is simulated as a single-phase homogeneous fluid. Therefore, the velocity and temperature difference between the solid and liquid phases is neglected. Thermophysical properties of the nanoparticles and the base liquid are gathered in Table 1. The flow is considered to be steady, two dimensional and laminar, and the radiation effects are negligible. The density variation in the nanofluid is approximated by the standard Boussinesq approximation. Furthermore, it is assumed that the viscous dissipation and Joule heating are neglected.

Therefore, governing equations can be written in dimensional form as follows:

$$\frac{\partial u}{\partial x}+\frac{\partial v}{\partial y}=0 \tag{1}$$

$$\rho_{nf}\left(u\frac{\partial u}{\partial x}+v\frac{\partial u}{\partial y}\right)=-\frac{\partial p}{\partial x}+\mu_{nf}\left(\frac{\partial^2 u}{\partial x^2}+\frac{\partial^2 u}{\partial y^2}\right) \tag{2}$$

$$\rho_{nf}\left(u\frac{\partial v}{\partial x}+v\frac{\partial v}{\partial y}\right)=-\frac{\partial p}{\partial y}+\mu_{nf}\left(\frac{\partial^2 v}{\partial x^2}+\frac{\partial^2 v}{\partial y^2}\right)+(\rho\beta_T)_{nf}g(T-T_c) \tag{3}$$

$$u\frac{\partial T}{\partial x}+v\frac{\partial T}{\partial y}=\alpha_{nf}\left(\frac{\partial^2 T}{\partial x^2}+\frac{\partial^2 T}{\partial y^2}\right) \tag{4}$$

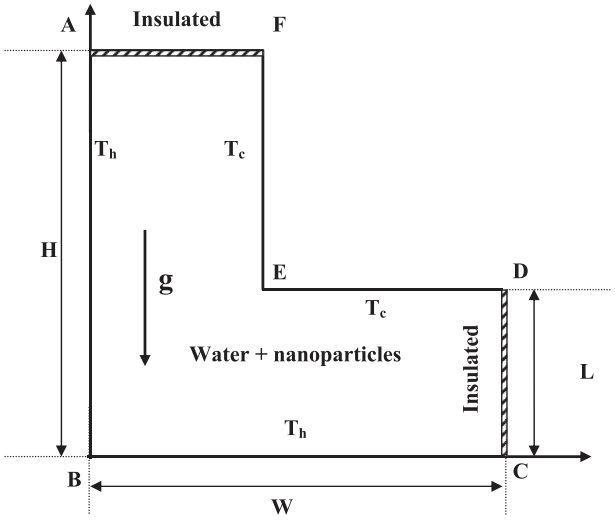

Fig. 1. Geometry of the problem.

Table 1
Thermo physical properties of fluid and nanoparticles.

Physical Properties	Fluid phase (Water)	Cu (nanoparticles)
C_p (J/kgK)	4179	385
ρ (kg/m^3)	997.1	8933
k (W/mK)	0.631	400
β × 10^{-5} (1/K)	21	1.6

The classical models reported in the literature are used to determine the properties of the nanofluid [42]:

$$\rho_{nf}=(1-\phi)\rho_f+\phi\rho_p \tag{5}$$

$$(\rho C_p)_{nf}=(1-\phi)(\rho C_p)_f+\phi(\rho C_p)_p \tag{6}$$

$$(\rho\beta)_{nf}=(1-\phi)(\rho\beta)_f+\phi(\rho\beta)_p \tag{7}$$

$$\alpha_{nf}=\frac{k_{nf}}{(\rho C_p)_{nf}} \tag{8}$$

In the above equations ϕ is the solid volume fraction, ρ is the density, α is the thermal diffusivity, C_p is the specific heat at constant pressure and β is the thermal expansion coefficient. The effective dynamic viscosity and thermal conductivity of the nanofluid are defined respectively for spherical particles in [43,44] as given by Eqs. 9 and 10:

$$\mu_{nf}=\frac{\mu_f}{(1-\phi)^{2.5}} \tag{9}$$

$$k_{nf}=k_f\frac{k_P+2k_f-2\phi\left(k_f-k_P\right)}{k_P+2k_f+\phi\left(k_f-k_P\right)} \tag{10}$$

The above equations are non-dimensionalized by using the following dimensionless variables:

$$X=\frac{x}{L},\quad Y=\frac{y}{L},\quad U=\frac{uL}{\alpha_{nf}},\quad V=\frac{vL}{\alpha_{nf}},\quad \theta=\frac{T-T_c}{T_h-T_c},\quad P=\frac{pL^2}{\rho_{nf}\alpha_{nf}^2}$$
$$Pr=\frac{\nu_{nf}}{\alpha_{nf}},\quad Ra=\frac{g\beta(T-T_c)L^3}{\nu_f\alpha_f} \tag{11}$$

Then the non-dimensional governing equations are

$$\frac{\partial U}{\partial X}+\frac{\partial V}{\partial Y}=0 \tag{12}$$

$$U\frac{\partial U}{\partial X}+V\frac{\partial U}{\partial Y}=-\frac{\partial P}{\partial X}+\mathrm{Pr}^*\left(\frac{\partial^2 U}{\partial X^2}+\frac{\partial^2 U}{\partial Y^2}\right) \tag{13}$$

$$U\frac{\partial V}{\partial X}+V\frac{\partial V}{\partial Y}=-\frac{\partial P}{\partial Y}+\mathrm{Pr}^*\left(\frac{\partial^2 V}{\partial X^2}+\frac{\partial^2 V}{\partial Y^2}\right)+Ra^*Pr^*\theta \tag{14}$$

$$U\frac{\partial \theta}{\partial X}+V\frac{\partial \theta}{\partial Y}=\left(\frac{\partial^2 \theta}{\partial X^2}+\frac{\partial^2 \theta}{\partial Y^2}\right) \tag{15}$$

Where

$$\mathrm{Pr}^* = \frac{\mu_{nf}}{\mu_f}\frac{C_{p_{nf}}}{C_{p_f}}\frac{k_f}{k_{nf}}\mathrm{Pr}, \quad Ra^* = \frac{(\rho\beta)_{nf}}{(\rho\beta)_f}\frac{k_f}{k_{nf}}\frac{(\rho C)_{p_{nf}}}{(\rho C)_{p_f}}\frac{\mu_f}{\mu_{nf}}Ra \tag{16}$$

2.2. LBM natural convection simulation

The lattice Boltzmann method (LBM) has become an alternative and attractive approach to simulate numerous fluid flow problems. The LBM was originated from Ludwig Boltzmann's kinetic theory of gases. The fundamental idea is that fluids can be imagined as consisting of a large number of small particles moving with random motions. The exchange of momentum and energy is achieved through particle streaming and billiard-like particle collision. For the incompressible non isothermal problems, (LBM) utilizes two distribution functions f_i and g_i, for the flow and temperature fields respectively.

For the flow field:

$$f_i(\mathbf{x}+\mathbf{c_i}\Delta t, t+\Delta t) = f_i(\mathbf{x},t) - \frac{1}{\tau_\nu}\left(f_i(\mathbf{x},t) - f_i^{\mathrm{eq}}(\mathbf{x},t)\right) + \Delta t\mathbf{c_i}F_i \tag{17}$$

For the temperature field:

$$g_i(\mathbf{x}+\mathbf{c_i}\Delta t, t+\Delta t) = g_i(\mathbf{x},t) - \frac{1}{\tau_\alpha}\left(g_i(\mathbf{x},t) - g_i^{\mathrm{eq}}(\mathbf{x},t)\right) \tag{18}$$

where the discrete particle velocity vectors is defined by c_i. Δt denotes lattice time step which is set to unity. τ_ν and τ_α are the relaxation time for the flow and temperature fields, respectively.f_i^{eq} and g_i^{eq} are the local equilibrium distribution functions that have an appropriately prescribed functional dependence on the local hydrodynamic properties which are calculated with Eqs. 17 and 18 and for flow and temperature fields respectively.

$$f_i^{\mathrm{eq}} = \omega_i\rho\left[1 + \frac{3(\mathbf{c_i}\cdot\mathbf{u})}{c^2} + \frac{9(\mathbf{c_i}\cdot\mathbf{u})^2}{2c^4} - \frac{3\mathbf{u}^2}{2c^2}\right] \tag{19}$$

$$g_i^{\mathrm{eq}} = \omega_i' T\left[1 + 3\frac{\mathbf{c_i}\cdot\mathbf{u}}{c^2}\right] \tag{20}$$

u and ρ are the macroscopic velocity and density, respectively. c is the lattice speed which is equal to $\Delta x/\Delta t$ where Δx is the lattice space similar to the lattice time step Δt which is equal to unity, ω_i is the weighting factor for flow and ω_i' is the weighting factor for temperature. D2Q9 model for flow and D2Q4 model for temperature and concentration are used in this work. The weighting factors and the discrete particle velocity vectors are different for these two models and they are calculated with Eqs. 21–23 as follows:

For D2Q9

$$\omega_0 = \frac{4}{9}, \omega_i = \frac{1}{9} \quad \text{for i} = 1,2,3,4 \quad \text{and} \quad \omega_i = \frac{1}{36} \quad \text{for i} = 5,6,7,8 \tag{21}$$

$$\mathbf{c_i} = \begin{cases} 0\ , & i=0 \\ (\cos[(i-1)\pi/2], \sin[(i-1)\pi/2])c\ , & i=1,2,3,4 \\ \sqrt{2}(\cos[(i-5)\pi/2+\pi/4], \sin[(i-5)\pi/2+\pi/4])c\ , & i=5,6,7,8 \end{cases} \tag{22}$$

For D2Q4

The temperature weighting factor for each direction is equal to $\omega_i' = 1/4$.

$$\mathbf{c_i} = (\cos[(i-1)\pi/2], \sin[(i-1)\pi/2])c\ , \quad i = 1,2,3,4 \tag{23}$$

The kinematic viscosity ν and thermal diffusivity α are respectively related to the relaxation time by Eq. (24):

$$\nu = \left[\tau_\nu - \frac{1}{2}\right]{c_s}^2\Delta t\ , \quad \alpha = \left[\tau_\alpha - \frac{1}{2}\right]{c_s}^2\Delta t \tag{24}$$

Where c_s is the lattice speed of sound witch is equal to $c_s = c/\sqrt{3}$. In the simulation of natural convection, the external force term F_i appearing in Eq. (3) is given by Eq. (25):

$$F_i = \frac{\omega_i}{{c_s}^2}F\cdot c_i \tag{25}$$

The macroscopic quantitiesρ, u and T can be calculated respectively by equations 26–28.

$$\rho = \sum_i f_i \tag{26}$$

$$\rho u = \sum_i f_i\mathbf{c_i} \tag{27}$$

$$T = \sum_i g_i \tag{28}$$

2.3. Non-dimensional parameters

For natural convection the Boussinesq approximation is applied. To ensure that the code works in an incompressible regime, the characteristic velocity must be small compared to the fluid speed of sound. Hence, in simulation, Mach number should be less than Ma = 0.3. Therefore, for all the considered cases in the present study, Mach number is fixed as 0.1.

By fixing Rayleigh number, Prandtl number and Mach number, the viscosity and thermal diffusivity are calculated from the definition of these non dimensional parameters.

$$\nu_f = NMac_s\sqrt{\frac{\mathrm{Pr}}{\mathrm{Ra}}} \tag{29}$$

where N is the number of lattices in y-direction.

The Nusselt number can be expressed as:

$$Nu_l = \frac{hH}{k_f} \tag{30}$$

where the heat transfer coefficient is computed from:

$$h = \frac{q_w}{T_h - T_C} \tag{31}$$

The thermal conductivity of the nanofluid is expressed as:

$$k_{nf} = -\frac{q_w}{\partial T/\partial X} \tag{32}$$

Substituting Eqs. (31) and (32) into Eq. (30), and using the dimensionless quantities, the local Nusselt number along the left wall can be written as:

$$Nu_l = -\frac{k_{nf}}{k_f}\left(\frac{\partial\theta}{\partial X}\right)\Big|_{X=0} \tag{33}$$

The average Nusselt number is obtained by integrating the local Nusselt number along the heat source:

$$\overline{Nu_l} = -\frac{1}{H}\int_0^H \frac{k_{nf}}{k_f}\left(\frac{\partial\theta}{\partial X}\right)\Big|_{X=0} \tag{34}$$

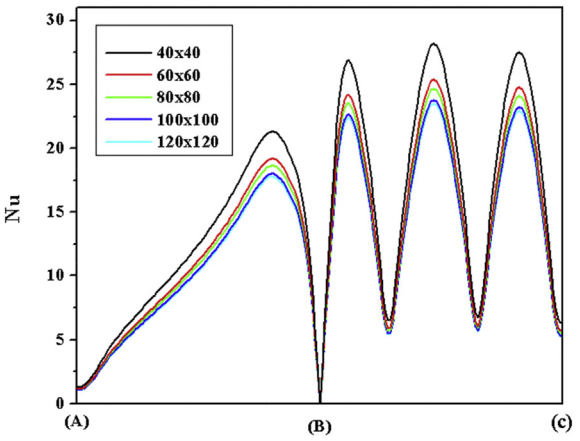

Fig. 2. Local Nu number on the hot walls (west wall (AB) and south wall (BC)) for different uniform grids with AR = 0.2 (Pr = 6.2, ϕ = 0.05 and Ra = 10^6).

3. Numerical method and validation

For grid independence study, the Local Nusselt number on the hot walls for $\phi = 0.05$ volume concentration nanofluid is calculated for AR = 0.2 at different lattice numbers (40×40, 60×60, 80×80, 100×100 and 120×120). The results are shown in Fig. 2. According to this figure, 100×100 lattices number is chosen as the final independent lattice numbers. For validation of the written computer code, the present numerical results for Cu/water nanofluid in L-shaped enclosure with AR = 0.2, ϕ = 0 and 0.05 at Ra = 10^6 are compared with results by Mohammad and Hossein [16]. For accurate comparison with each of the mentioned results, we use the nanofluid thermophysical properties that have been applied in the corresponding references. The comparison results

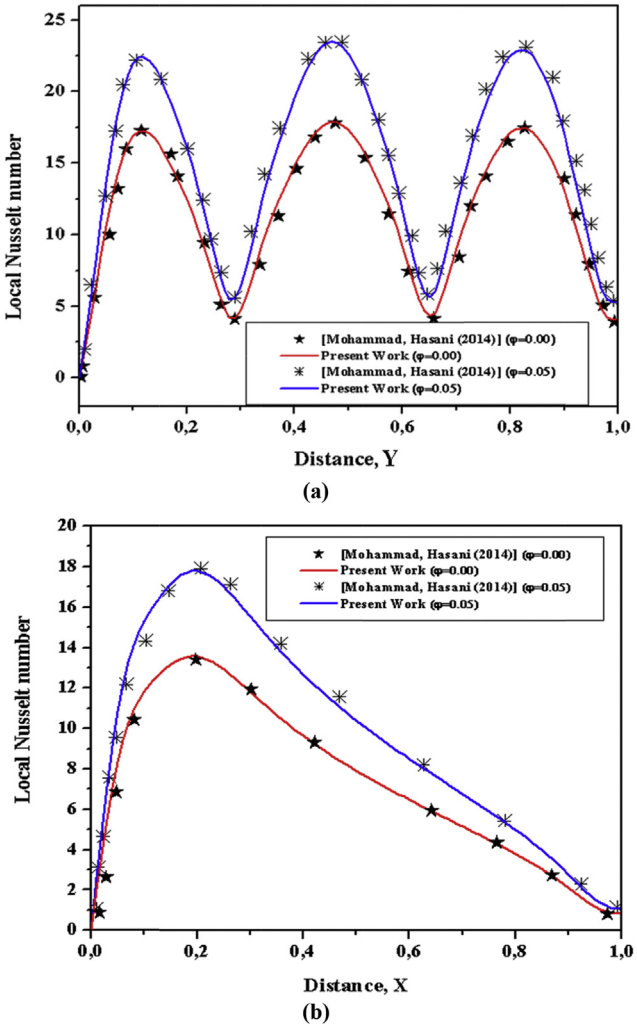

Fig. 3. Comparison between present code and Mohammad and Hasani [16] in the presence of nanofluid (AR = 0.2, ϕ = 0, ϕ = 0.05 and Ra = 10^6), (a) south wall (BC) and (b) west wall (AB).

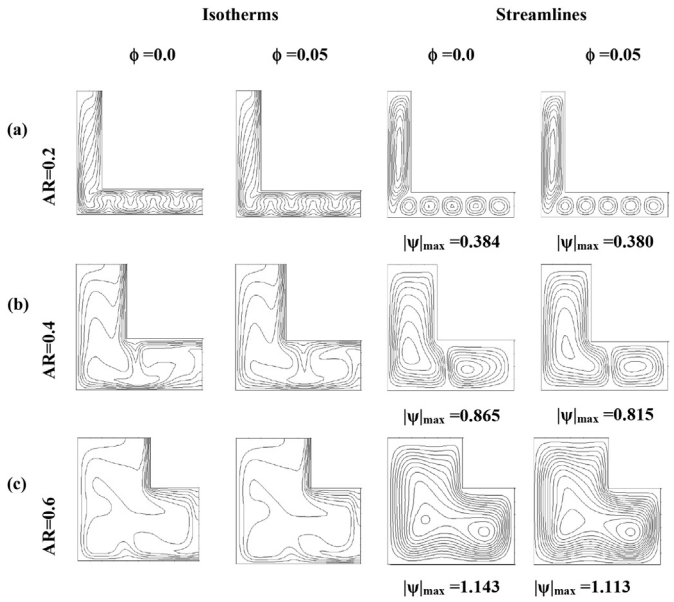

Fig. 4. Isotherms and Streamlines for ϕ = 0, ϕ = 0.05 at Ra = 10^6, (a) AR = 0.2, (b) AR = 0.4, (c) AR = 0.6.

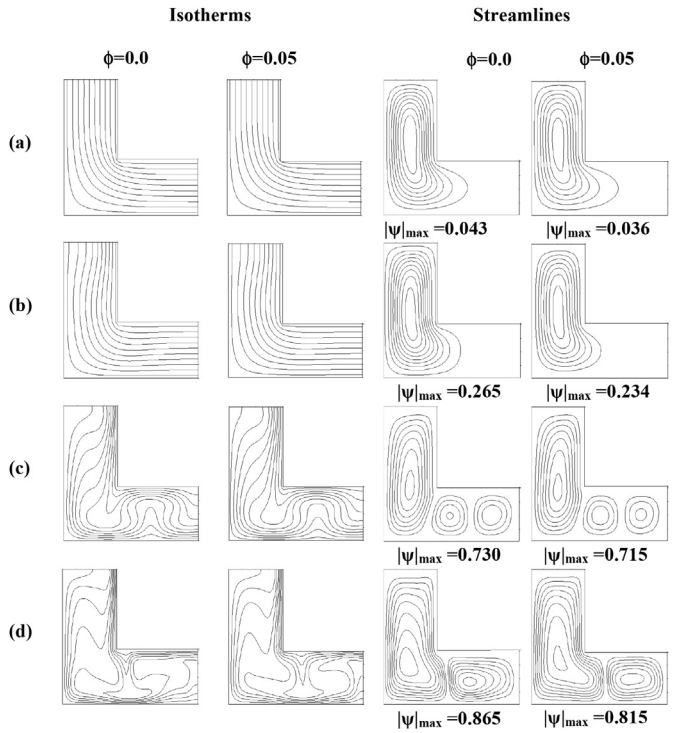

Fig. 5. Isotherms and Streamlines for ϕ = 0, ϕ = 0.05 with AR = 0.4, (a) Ra = 10^3, (b) Ra = 10^4, (c) Ra = 10^5, (d) Ra = 10^6.

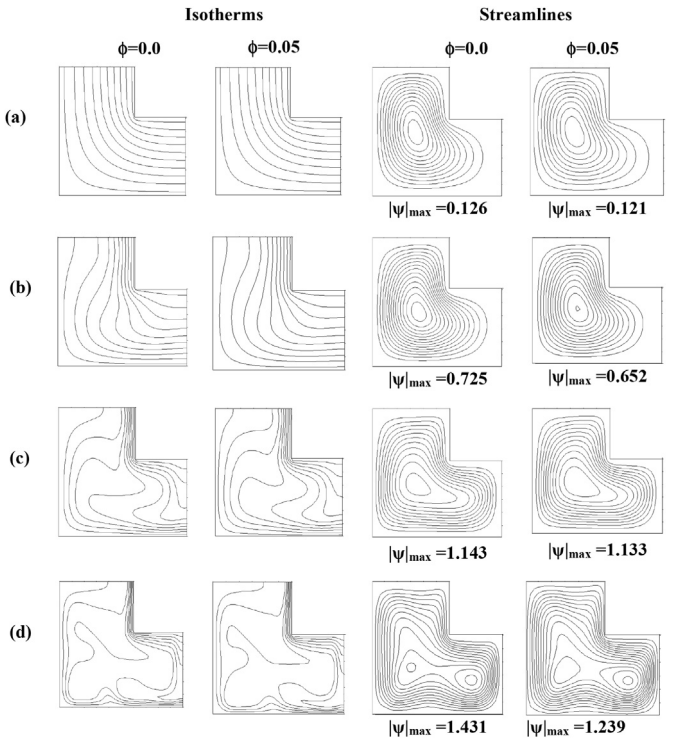

Fig. 6. Isotherms and Streamlines for $\phi = 0$, $\phi = 0.05$ with AR = 0.6, (a) Ra = 10^3, (b) Ra = 10^4, (c) Ra = 10^5, (d) Ra = 10^6.

are shown in Fig. 3. According to this figure, it is obvious that the agreement between the results is very good for all the Ra numbers. Based on the aforementioned comparisons, the developed code is reliable for studying natural convection of a nanofluid confined in an L-shaped enclosure.

4. Results and discussion

In this section, numerical results for Cu/water nanofluid free convection heat transfer in an L-shaped cavity is presented. The main goal is to investigate the effects of pertinent parameters such as Rayleigh number, nanoparticle volume concentration and aspect ratio of the L-shaped enclosure on the flow and temperature fields. The variation range for Rayleigh number, nanoparticle concentration and aspect ratio are 10^3–10^6, 0–0.05 and 0.2–0.6, respectively.

Fig. 4, illustrates the effect of increase in AR (AR = 0,2; 0,4; 0,6) on flow pattern and temperature distribution inside the enclosures filled with pure fluid ($\phi = 0$) and nanofluid ($\phi = 0{,}05$) at Ra = 10^6. As can be seen from the streamlines in this figure, for AR = 0.2 the fluid is heated by the hot walls and expands as it moves upward. Then the fluid is cooled by the cold walls (DE and EF) and compressed as it moves downward. Hence, a clockwise eddy is established in the whole portion of the enclosure. In the horizontal part of the cavity five eddies are formed and rotating in opposing directions. This part is similar to the problem of natural convection in an enclosure heated from below and cooled from above with large aspect ratio. The isotherms for this aspect ratio are condensed near the walls in the vertical part of the cavity and oscillating in the horizontal part of the L shaped enclosure. For AR = 0.4 the eddy breaks into two

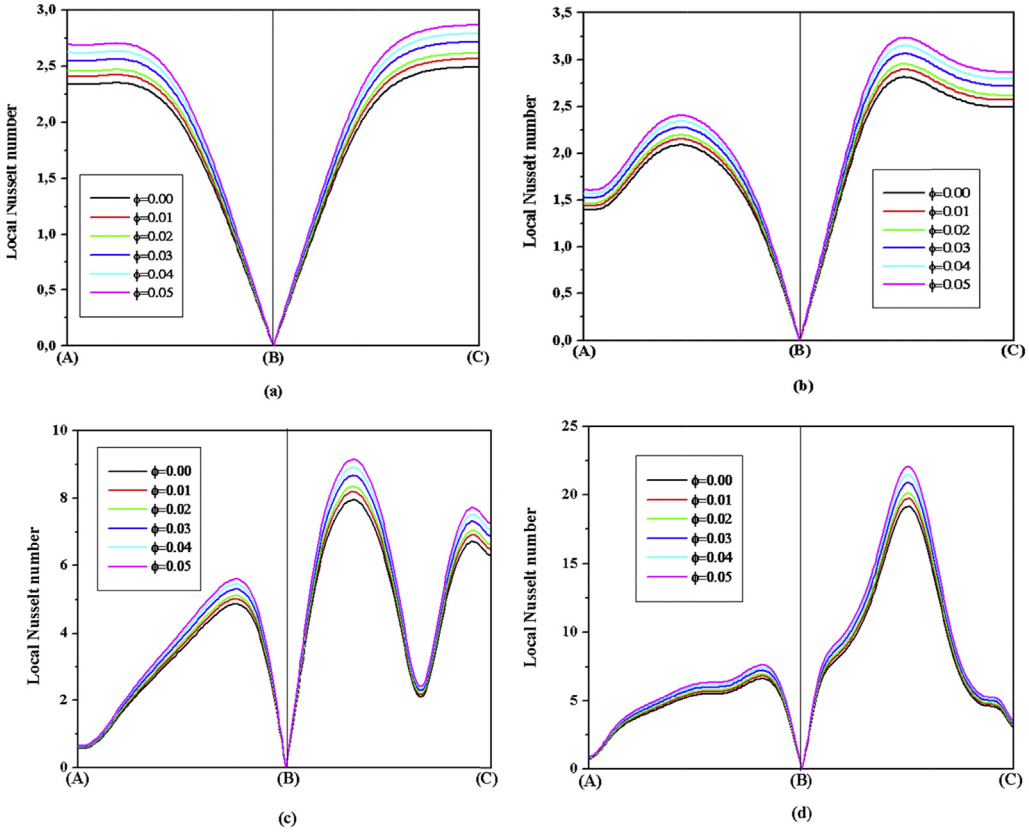

Fig. 7. Nanoparticle volume concentration effect on the local Nu number on the hot walls (west wall (AB) and south wall (BC)) with AR = 0.4 (a) Ra = 10^3, (b) Ra = 10^4, (c) Ra = 10^5 and (d) Ra = 10^6.

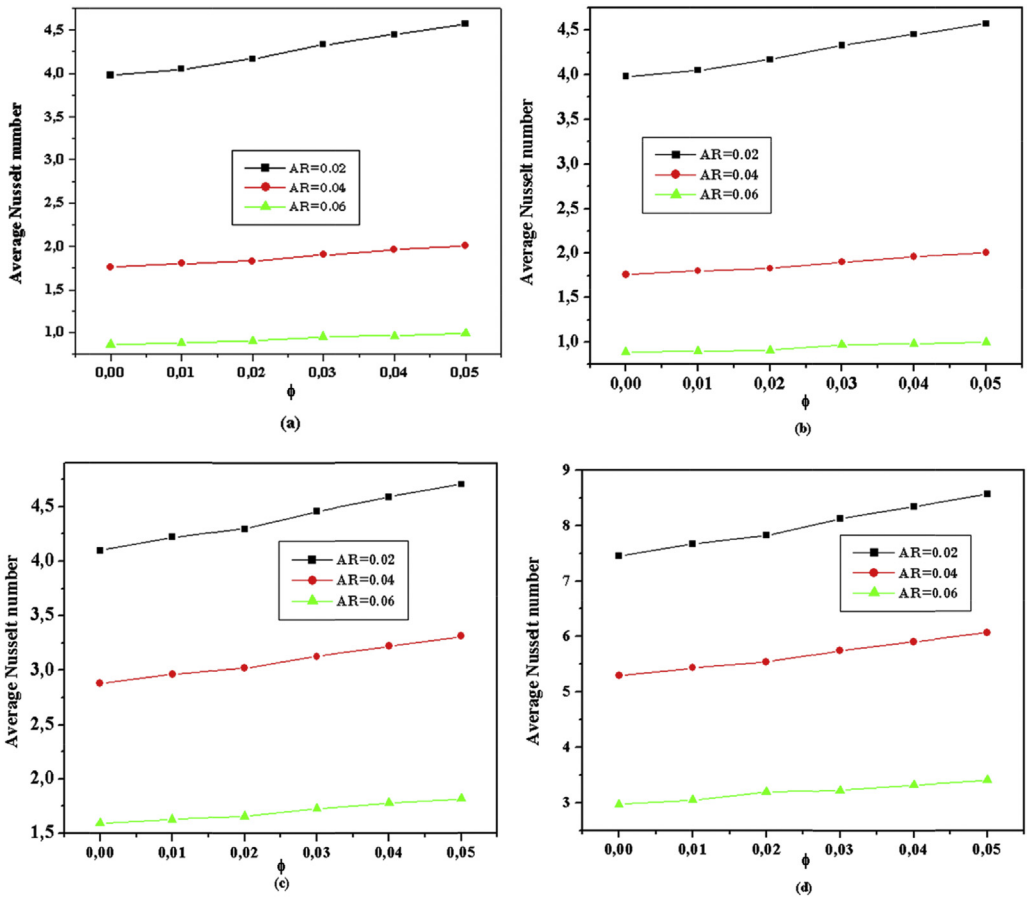

Fig. 8. Nanoparticle volume concentration effect on the average Nu number on the hot west wall (AB), (a) Ra = 10^3, (b) Ra = 10^4, (c) Ra = 10^5 and (d) Ra = 10^6.

counter-rotating eddies. The bigger eddy is clockwise and is located in the left side of the enclosure while the smaller counterclockwise eddy is located under the cold rib. For AR = 0.6, two eddies are developed under the cold rib. The right hand side and the left hand side eddies are clockwise and counterclockwise, respectively. Using a nanofluid would reduce the strength of flow in the cavity. In fact, the addition of the nanoparticles attenuates considerably the distortions exhibited by the streamlines of the pure fluid in the vicinity of the center of the main flow cell. The intensity of these cells, characterized by $|\psi_{max}|$, increases with the Rayleigh number and decreases as the nanoparticle volume concentration increases. This can be explained by the fact that the viscosity of the nanofluids increases with the volume fraction. On the other hand, as mentioned before because of large conductivity coefficient of nanoparticle comparing to conductivity coefficient of the base fluid, using nanofluid will amplify the conductive heat transfer mechanism in the cavity. Thus, by using nanofluids, heat transfer characteristics in the cavity can be enhanced or reduced and the result depends if the conductive effects of nanofluid or convective effects of nanofluid are dominant.

Streamlines and isotherms for nanofluid free convection in an L-shaped enclosure with AR = 0.4 at different Ra and ϕ are shown in Fig. 5. As it is clear in Fig. 5, for pure water flow at Ra = 10^3 and 10^4, there is a clockwise vortex in the vertical part of the cavity. The maximum stream function magnitude occurs in the central core of the L-shaped enclosure. Even though the global flow structure is not considerably affected by the addition of the Cu nanoparticles, the global intensity of the flow cells may be significantly modified (depending on Ra) by changing the concentration of the nanoparticles. On the other hand, the streamlines, do not take place under the cold rib. It is because of existence of small gap between the hot bottom wall and the cold rib which limits the flow movement. At Ra = 10^5 two vortexes are formed in the horizontal part of the L-shaped enclosure. Further increasing the Ra to 10^6, the two vortexes in the horizontal part coalesce to make a larger and stronger counter-clockwise vortex. The streamline patterns for other concentrations are the same more or less, but, the stream function magnitude decreases with concentration. Non-dimensional isotherms are shown in this figure. For water flow and nanofluids at Ra = 10^3–10^4, the isotherms are formed parallel to the cavity walls which, as described before, implies a heat transfer by conduction. But, when the Ra increases, the isotherms change considerably and heat transfer by convection dominates.

Fig. 6 shows the Cu/water nanofluid streamlines and isotherms for L-shaped enclosure with AR = 0.6 of nanofluid ($\phi = 0.05$) and pure fluid ($\phi = 0$). As it can be seen from Fig. 6, at Ra = 10^3 for pure water flow ($\phi = 0$), a clockwise vortex with elliptical core is formed in the cavity. Also, the maximum stream function magnitude occurs in the central core of the cavity. But, increasing the Ra from 10^3 to 10^5 for water flow, the streamlines extend to the whole channel and occupy the horizontal part of the cavity. Increasing the Ra number, the buoyancy force enhances which in turn increases the stream function magnitude. For Ra = 10^6, two secondary vortexes are seen inside the primary vortex. Also, when the nanofluid concentration increases, the streamline pattern does not change considerably (especially for smaller Ra), but, its effect on decreasing the maximum stream function is clear. This can be explained due to the increase in the nanofluid viscosity. For Ra = 10^3 and in all the volume concentrations, the isotherms are parallel to the enclosure walls that implies conduction heat transfer in the cavity. For higher

Rayleigh numbers, the isotherms are not parallel to the walls and distinct thermal boundary layers are formed near the vertical walls that show the domination of the free convection heat transfer compared to the heat conduction.

Fig. 7 shows the local Nusselt number on the hot walls (AB, BC) for AR = 0.4, and different volume concentration and Rayleigh numbers. It is clear that in all the Ra numbers, the local Nusselt number increases with an increase in the nanoparticle volume concentration. The reason is high thermal conductivity of copper nanoparticles, which enhances conductive heat transfer mechanism. According to Fig. 7 (a) since there are no vortexes in the horizontal part and so the heat conduction mode dominates, the local Nu number profiles vary smoothly in this region. This figure shows that the local Nusselt number on the left vertical wall is identical to those on the bottom wall for the conduction regime represented by $Ra = 10^3$. This can be explained by the fact of the symmetric positions between AB and BC. By increasing Ra from 10^3 to 10^4, the maximum of the Nusselt number on the bottom wall undergoes some improvement; its value passes from 2.8 to 3.2 following this increase of Ra (Fig. 7 (b)). But, on the contrary, along the bottom wall, the maximum of the Nusselt number is decreased; its value passes from 2.7 to 2.4. However, at $Ra = 10^5$ Fig. 7 (c and d), the vortexes in the horizontal part, makes oscillations in the local Nu profile.

Fig. 8 shows the average Nu number on the hot wall for different volume concentration, Rayleigh numbers and aspect ratios. It is seen that the heat transfer is always improved by increasing the nanoparticles fraction, but the rate of improvement depends on Ra. More precisely, for $Ra = 10^3, 10^4, 10^5, 10^6$, the average Nu number increases respectively by 15.93%, 16.54%, 16.75% and 17.33% when the volume fraction of nanoparticles ϕ is increased from 0 to 0.05. We remark also from the curves of Fig. 8 that the average Nu number exhibits a quasi linear variation with the parameter ϕ. Finally, the slope of the lines increases with a decrease in the aspect ratio. It means that the heat transfer increases by volume concentration is more pronounced for lower aspect ratios.

5. Conclusions

The lattice Boltzmann method is used to investigate the Cu/water nanofluid free convection heat transfer in an L-shaped enclosure. The effects of the pertinent parameters such as Rayleigh number, aspect ratio and nanoparticle volume concentration on the thermal and fluid fields are investigated. The following main conclusions can be made according to the numerical results:

- In all the considered Ra and AR, increasing the nanoparticle volume concentration increases the average Nusselt number.
- The aspect ratio of the L-shaped enclosure has significant effect on the streamlines and temperature fields.
- Decreasing the aspect ratio, transition point from conduction to free convection heat transfer modes is postponed to higher Ra numbers.
- The rate of the heat transfer enhancement with volume concentration is higher for lower aspect ratios.
- The vortexes in the horizontal part of the cavity result in an oscillatory local Nusselt number in that region.

References

[1] M. Dalavar, M. Farhadi, K. Sedighi, Effect of the heater location on heat transfer and entropy generation in the cavity using the lattice Boltzmann method, Heat Transf. Res. 40 (2009) 505–519.

[2] E. Fattahi, M. Farhadi, K. Sedighi, Lattice Boltzmann simulation of natural convection heat transfer in eccentric annulus, Int. J. Therm. Sci. 49 (2010) 2353–2362.

[3] H. Nemati, M. Farhadi, K. Sedighi, E. Fattahi, A.A. Rabienataj, Lattice Boltzmann simulation of nanofluid in lid-driven cavity, Int. Commun. Heat. Mass Transf. 37 (2010) 1528–1534.

[4] M. Mahmodi, S.M. Hashemi, Numerical study of natural convection of a nanofluid in C-shaped enclosures, Int. J. Therm. Sci. 55 (2012) 76–89.

[5] M.M. Rashidi, S. Abelman, N. Freidooni Mehr, Entropy generation in steady MHD flow due to a rotating porous disk in a nanofluid, Int. J. Heat. Mass Transf. 62 (2013) 515–525.

[6] H.R. Ashorynejad, A.A. Mohamad, M. Sheikholeslami, Magnetic field effects on natural convection flow of a nanofluid in a horizontal cylindrical annulus using Lattice Boltzmann method, Int. J. Therm. Sci. 64 (2013) 240–250.

[7] U. S. Choi, Enhancing thermal conductivity of fluids with nanoparticles, developments and application of non-Newtonian flows, ASME 66 (1995) 99–105.

[8] K. Khanafer, K. Vafai, M. Lightstone, Buoyancy-driven heat transfer enhancement in a two dimensional enclosure utilizing nanofluid, Int. J. Heat. Mass Transf. 46 (2003) 3639–3653.

[9] F.H. Lai, Y.T. Yang, Lattice Boltzmann simulation of natural convection heat transfer of Al_2O_3/water nanofluids in a square enclosure, Int. J. Therm. Sci. 50 (2011) 1930–1941.

[10] C.J. Ho, W.K. Liu, Y.S. Chang, Numerical study of natural convection of a nanofluid in C-shaped enclosures, Int. J. Therm. Sci. 49 (2010) 1345–1353.

[11] Z. Alloui, P. Vasseur, M. Reggio, Natural convection of nanofluids in a shallow cavity heated from below, Int. J. Therm. Sci. 50 (2011) 385–393.

[12] Y. He, C. Qi, Y. Hu, Lattice Boltzmann simulation of alumina–water nanofluid in a square cavity, Nanoscale Res. Lett. 184 (2011) 1–8.

[13] K. Kahveci, Buoyancy driven heat transfer of nanofluids in a tilted enclosure, Int. J. Heat. Mass Transf. 132 (2010) 062501.

[14] M. Mahmoodi, Numerical simulation of free convection of a nanofluid in L-shaped cavities, Int. J. Therm. Sci. 50 (2011) 1731–1740.

[15] R. Dehnavi, A. Rezvani, Numerical investigation of natural convection heat transfer of nanofluids in a Γ-shaped cavity, Superlattices Microstruct. 52 (2012) 312–325.

[16] M. Kalteh, H. Hasani, Lattice Boltzmann simulation of nanofluid free convection heat transfer in an L-shaped enclosure, Superlattices Microstruct. 66 (2014) 112–128.

[17] A. Mahmoudi, I. Mejri, M.A. Abbassi, A. Omri, Lattice Boltzmann simulation of MHD natural convection in a nanofluids-filled cavity with linear temperature distribution, Powder Technol. 256 (2014) 257–271.

[18] M.A.Y. Bakier, Flow in open C-shaped cavities: how far does the change in boundaries affect nanofluid? Eng. Sci. Technol. Int. J. 17 (2014) 116–130.

[19] I. Mejri, A. Mahmoudi, M.A. Abbassi, A. Omri, Magnetic field effect on entropy generation in a nanofluid-filled enclosure with sinusoidal heating on both side walls, Powder Technol. 266 (2014) 340–353.

[20] M. Sheikholeslami, M. Gorji-Bandpy, D.D. Ganji, Numerical investigation of MHD effects on Al_2O_3-water nanofluid flow and heat transfer in a semi-annulus enclosure using LBM, Energy 60 (2013) 501–510.

[21] M. Sheikholeslami, M. Gorji-Bandpy, K. Vajravelu, Lattice Boltzmann simulation of magnetohydrodynamic natural convection heat transfer of Al_2O_3–-water nanofluid in a horizontal cylindrical enclosure with an inner triangular cylinder, Int. J. Heat. Mass Transf. 80 (2015) 16–25.

[22] M. Sheikholeslami, D.D. Ganji, Entropy generation of nanofluid in presence of magnetic field using Lattice Boltzmann method, Phys. A 417 (2015) 273–286.

[23] M. Sheikholeslami, M. Gorji-Bandpy, R. Ellahi, A. Zeeshan, Simulation of MHD CuO–water nanofluid flow and convective heat transfer considering Lorentz forces, J. Magnetism Magnetic Mater. 369 (2014) 69–80.

[24] M. Sheikholeslami, M. Gorji-Bandpy, D.D. Ganji, MHD free convection in an eccentric semi-annulus filled with nanofluid, J. Taiwan Inst. Chem. Eng. 45 (2014) 1204–1216.

[25] M. Sheikholeslami, D.D. Ganji, M.Y. Javed, R. Ellahi, Effect of thermal radiation on magnetohydrodynamics nanofluid flow and heat transfer by means of two phase model, J. Magnetism Magnetic Mater. 374 (2015) 36–43.

[26] R. Ellahi, The effects of MHD and temperature dependent viscosity on the flow of non-Newtonian nanofluid in a pipe: analytical solutions, Appl. Math. Model 37 (3) (2013) 1451–1467.

[27] A.K. Hussein, H.R. Ashorynejad, M. Shikholeslami, S. Sivasankaran, Lattice Boltzmann simulation of natural convection heat transfer in an open enclosure filled with Cu–water nanofluid in a presence of magnetic field, Nucl. Eng. Des. 268 (2014) 10–17.

[28] G.H.R. Kefayati, Natural convection of ferrofluid in a linearly heated cavity utilizing LBM, J. Mol. Liq. 191 (2014) 1–9.

[29] M.M. Rahman, H.F. Öztop, S. Mekhilef, R. Saidur, K. Al-Salem, Unsteady natural convection in Al_2O_3–water nanoliquid filled in isosceles triangular enclosure with sinusoidal thermal boundary condition on bottom wall, Superlattice, Microst 67 (2014) 181–196.

[30] A. Mahmoudi, I. Mejri, M.A. Abbassi, A. Omri, Analysis of MHD natural convection in a nanofluids filled open cavity with non uniform boundary condition in the presence of uniform heat generation/absorption, Powder Technol. 269 (2015) 275–289.

[31] S. Mukhopadhyay, I.C. Mandal, Magnetohydrodynamic (MHD) mixed convection slip flow and heat transfer over a vertical porous plate, Eng. Sci. Technol. Int. J. 18 (2015) 98–105.

[32] G.H. Kefayati, Effect of a magnetic field on natural convection in an open cavity subjugated to water/alumina nanofluid using Lattice Boltzmann method, Int. Commun. Heat. Mass Transf. 40 (2013) 67–77.

[33] G.H. Kefayati, Lattice Boltzmann simulation of MHD natural convection in a nanofluid-filled cavity with sinusoidal temperature distribution, Powder Technol. 243 (2013) 171–183.

[34] M. Sheikholeslami, S. Abelman, D.D. Ganji, Numerical simulation of MHD nanofluid flow and heat transfer considering viscous dissipation, Int. J. Heat. Mass Transf. 79 (2014) 212–222.
[35] M. Sheikholeslami, M. Gorji-Bandpay, D.D. Ganji, Investigation of nanofluid flow and heat transfer in presence of magnetic field using KKL model, Arab. J. Sci. Eng. 39 (6) (2014) 5007–5016.
[36] M. Sheikholeslami, D.D. Ganji, Heated permeable stretching surface in a porous medium using nanofluids, J. Appl. Fluid Mech. 7 (3) (2014) 535–542.
[37] M. Sheikholeslami, D.D. Ganji, M. Gorji-Bandpy, S. Soleimani, Magnetic field effect on nanofluid flow and heat transfer using KKL model, J. Taiwan Inst. Chem. Eng. 45 (2014) 795–807.
[38] M. Sheikholeslami, M. Gorji-Bandpy, D.D. Ganji, Natural convection in a nanofluid filled concentric annulus between an outer square cylinder and an inner elliptic cylinder, Sci. Iran. Trans. B: Mech. Eng. 20 (4) (2013) 1241–1253.
[39] M. Sheikholeslami, M. Gorji-Bandpy, G. Domairry, Free convection of nanofluid filled enclosure using lattice Boltzmann method (LBM), Appl. Math. Mech. Engl. 34 (7) (2013) 1–15.
[40] M. Sheikholeslami, M. Gorji-Bandpy, D.D. Ganji, Lattice Boltzmann method for MHD natural convection heat transfer using nanofluid, Powder Technol. 254 (2014) 82–93.
[41] M. Sheikholeslami, M. Gorji-Bandpay, D.D. Ganji, Magnetic field effects on natural convection around a horizontal circular cylinder inside a square enclosure filled with nanofluid, Int. Commun. Heat. Mass Transf. 39 (7) (2012) 978–986.
[42] Y. Xuan, W. Roetzel, Conceptions for heat transfer correlation of nanofluids, Int. J. Heat Mass Transf. 19 (2000) 3701–3707.
[43] H.C. Brinkman, The viscosity of concentrated suspensions and solution, J. Chem. Phys. 20 (1952) 571–581.
[44] M. Garnett, A Treatise on Electricity and Magnetism, vol. 54, Oxford University Press, Cambridge, 1873.